



Solvent contribution to ferrocene conformation: Theory and experiment

Feng Wang^{a,*}, Shawkat Islam^a, Christopher T. Chantler^b^a Department of Chemistry and Biotechnology, School of Science, Computing and Engineering Technologies, Swinburne University of Technology, Hawthorn, Victoria, 3122, Australia^b School of Physics, University of Melbourne, Parkville, Victoria, 3052, Australia

ARTICLE INFO

Keywords:

Ferrocene conformers

Solvent effects

IR spectrum

Energy decomposition analysis

Theory and experiment

ABSTRACT

Solvent impacts on ferrocene configuration and the nature of its component energies. The measured infrared (IR) spectra of ferrocene (Fc) in the region 400–500 cm^{-1} exhibit very different profiles in gas phase and in solutions. The present study further explores such the differences in gas phase and in solutions using combined theoretical calculations and experimental measurements. It concentrates on the IR spectra in the region of 400–1200 cm^{-1} using non-polar (tetrachloromethane (CCl₄) and n-hexane (Hex)) and polar (acetonitrile (ACN), dichloromethane (DCM), tetrahydrofuran (THF) and 1,4-dioxane (DOX)) solvents. Six relatively intense normal modes in this region (ν_7 , $\nu_{8,9}$, ν_{18} , $\nu_{22,23}$, $\nu_{30,31}$ and ν_{37} at approximately 482, 495, 815, 840, 1006, 1110 cm^{-1}) were obtained. The dependence of the relative energies of the eclipsed and staggered rotamers of Fc on the polarity of the solvent is small. Analysis of the band profile for the vibrational modes in the 480–500 cm^{-1} region (ν_7 , $\nu_{8,9}$) using the reaction coordinate model suggests that the energy difference between the eclipsed and staggered rotamers ($\Delta E_{e-s \text{ solv}}$) may be underestimated by implicit solvent model in the calculations. Further investigation in this direction is warranted. The impact of solvation on Fc configuration is further investigated using energy decomposition analysis (EDA) in a non-polar (tetrachloromethane (CCl₄)) and a polar (acetonitrile (ACN)) solvent. These calculations suggest that solvation substantially changes the electrostatic and quantum mechanical Pauli energy contributions to the interaction energy of Fc conformers, which result in a large steric energy in solvents to enhance the dominance of the eclipsed Fc, an observation consistent with the analysis of the bands due to the ν_7 and $\nu_{8,9}$ vibrational modes.

1. Introduction

Conformational change is an underlying feature of the chemical reactions of complex molecules. It is therefore important that we make an assessment of the ability of computational methods to satisfactorily deal with this contribution to the energetics of chemical reactions. Of interest in this contribution is the role of solvent as well as the performance of different implicit solvation models commonly used in density functional theory (DFT) calculations. The IR spectroscopy and dynamics related to interconversion between the rotameric forms of ferrocene (di-cyclopentadienyl iron, FeCp₂ or Fc) is an important example (Fischer and Pfab, 1952; Wang et al., 2021; Wilkinson et al., 1952). Fc is among the most recognisable molecules in science (Seeman and Cantrill, 2016), due to the unusual structure and bonding (Dunitz and Orgel, 1955; Dunitz, 1993; Coriani et al., 2006), the low-energy difference and subsequent interconversion dynamics (Fischer and Pfab, 1952; Wang et al., 2021; Wilkinson et al., 1952) between the high-symmetry conformers

(Haaland and Nilsson, 1968; Kubo et al., 1981; Appel et al., 2015) and the extensive range of applications dependent on molecules having the Fc core structure (Pietschnig, 2016; Larik et al., 2017; Yu and Shi, 2017; Zhao et al., 2017; Hao et al., 2018). In particular, different independent methods have confirmed that the D_{5h} conformation is lowest in energy (Bohn and Haaland, 1966; Seiler and Dunitz, 1979; Bourke et al., 2016). The stable form and the energy difference between the eclipsed and staggered forms can be obtained from analysis of the IR spectrum (Best et al., 2016; Trevorah et al., 2020; Islam et al., 2017) and synchrotron based X-ray absorption fine structure (XAFS) (Bourke et al., 2016; Chantler et al., 2012; Islam et al., 2016).

The small calculated energy difference between the D_{5h} and D_{5d} forms of Fc is a feature of published ab initio studies and the value of 0.58 kcal·mol⁻¹, obtained from DFT calculations (B3LYP/m6-31G(d)) (Mohammadi et al., 2012) is consistent with experimental estimates for the gas-phase species (Haaland and Nilsson, 1968). More recent work has demonstrated that the spectra show a large temperature dependence

* Corresponding author.

E-mail address: fwang@swin.edu.au (F. Wang).<https://doi.org/10.1016/j.radphyschem.2021.109697>

Received 28 April 2021; Received in revised form 24 June 2021; Accepted 25 June 2021

Available online 9 July 2021

0969-806X/© 2021 Elsevier Ltd. All rights reserved.

of the IR spectra of dynamic molecules, such as Fc, sensitive to the energy barrier (Best et al., 2016; Wang and Vasilyev, 2020; Islam et al., 2017). For Fc the sensitivity of the band profile in the 400-500 cm^{-1} region, arising from the ν_7 and $\nu_{8,9}$ normal modes, provides a signature of the lowest energy form and the energy difference between the different rotameric forms (Best et al., 2016; Lippincott and Nelson, 1958; Trevorah et al., 2020). Thus, Fc provides an excellent model system for investigating the impact of the solvent environment on the molecular dynamics and the performance of computational methods to provide insight into those processes.

The nature of the solvent can affect molecular energies, structures and properties. The DFT calculations using appropriately selected basis sets predict correctly IR spectra of both D_{5h} and D_{5d} forms and spectra (Mohammadi et al., 2012) and therefore, can be used to calculate the temperature dependence of the band profiles (Best et al., 2016). Different investigations of Fc have significantly different rotation barriers (as measured by NMR (Kubo et al., 1981; Kubo et al., 1986), inelastic neutron scattering (Kemner et al., 2000) and quasi-elastic neutron scattering (Appel et al., 2015) techniques) claimed to range from ca. 1–6 $\text{kcal}\cdot\text{mol}^{-1}$. The sensitivity of the rotation barrier to the molecule-molecule interactions of the crystalline structure suggests that solute-solvent interactions may have similarly large impacts on the dynamics of Fc in solution. In view of the impact that solvation has on the energetics and reactivity of molecular species, it is important to investigate solvent contributions in the measurements of IR profile of Fc.

Implicit continuum solvation models have been developed over many years and have provided computationally efficient solutions to this problem (Ribeiro et al., 2011). In these implicit solvent models, the bulk of the solvent is represented as a structureless polarizable medium characterized primarily by its dielectric constant, ϵ , such as in the polarizable continuum model (PCM) (Cossi and Barone, 1998; Amovilli et al., 1998) and the conductor-like screening model (COSMO) (Klamt and Schuurmann, 1993; Klamt, 1995; Klamt and Jonas, 1996; Pye and Ziegler, 1999). Despite the non-molecular nature of the approach, the continuum picture remains very useful, and often necessary, to account for long range interactions (Mennucci, 2010). In the present study, we investigate solvent effects on the relative energies of the D_{5h} and D_{5d} conformers of Fc in a number of organic solvents. We further explore nature of the energies of Fc conformers in solvents using the energy decomposition analysis (EDA) (von Hopffgarten and Frenking, 2012), in order to obtain insight into the solute-solvent interactions which lead to the dominance of D_{5h} Fc conformer in solutions.

2. Experimental and theoretical methods

In addition to the Fc IR measurements in four different solvents, i.e., acetonitrile (ACN), dichloromethane (DCM), tetrahydrofuran (THF) and 1,4-dioxane (DOX) which are detailed in the same issue Wang et al. (2021) together with the Fc IR spectra in two non-polar solvents of tetrachloromethane (CCl_4), and n-hexane (Hex) in the same conditions, measured earlier (Best et al., 2016). For details please refer to Wang et al. (2021) and Best et al. (2016)

The quantum mechanical calculations for Fc (both conformers) were performed with the DFT B3LYP/m6-31G(d) model (Mitin et al., 2003), as employed previously (Mohammadi et al., 2012; Best et al., 2016). Newer models including a modification for long-range interactions such as CAM-B3LYP/m6-31G(d) (Yanai et al., 2004), and D3 Grimme's dispersion correction (Grimme et al., 2010) such as B3LYP-D3 and CAM-B3LYP-D3 models are also employed in the calculations. No IR scaling factors are employed in the calculations.

The energy decomposition analysis (EDA) based extended transition state (ETS) scheme is applied to Fc in CCl_4 and ACN solutions in which the B3LYP/TZ2P + model (Chong et al., 2004) and COSMO method (Klamt and Schuurmann, 1993; Klamt, 1995; Klamt and Jonas, 1996; Pye and Ziegler, 1999) are employed. The same EDA fragmental scheme in gas phase (Wang et al., 2015) is employed in solvents in the present

study. The CCl_4 solvent was selected since the Fc IR spectra was also measured earlier by Lippincott and Nelson (1958) for comparison and validation purposes. The polar ACN solvent was selected to compare with a non-polar solvent. Calculations used the computational chemistry packages Gaussian (Frisch et al., 2009) and Amsterdam Density Functional (ADF) (Baerends et al., 2016).

3. Results and discussion

3.1. Model effects on the calculated IR spectra of Fc

Computational treatment of solvation effects includes implicit solvent continuum models. Implicit solvent models such as the polarizable continuum model (PCM) (Cossi and Barone, 1998), the conductor PCM (CPCM, which approximates the volume polarization) (Cossi et al., 2003; Barone and Cossi, 1998) and the solute molecule density (SMD) model (Marenich et al., 2009) were employed for the IR spectral calculations of the Fc conformers. Geometry optimisation of solvated Fc in all cases predict geometries close to D_{5h} , in some cases with a small distortion as reflected by imaginary frequencies calculated for ν_1 for both the D_{5h} and D_{5d} forms. The selected properties of eclipsed and staggered Fc conformers calculated using PCM are given in Table S1. The magnitude of the distortion depends on the solvation model and most likely reflects a mismatch between the symmetry of the solvent-excluded cavity and the molecular symmetry. The SMD model gives a more pronounced distortion with the symmetry of the eclipsed Fc conformer lowered from D_{5h} to C_s in all solvents except DOX and Hex, and the symmetry of the staggered Fc is lowered from D_{5d} to C_i in DCM and THF. The PCM model, however, consistently predicts the lowest symmetry form to have D_{5h} symmetry and the highest energy form having D_{5d} symmetry for all solvents. The predictions of the different solvation models in terms of the dependence of the relative energies of the Fc conformers ($\Delta(\Delta E_{e-s,\text{solv}}) = (E_{e,\text{solv}} - E_{s,\text{solv}}) - (E_{e,\text{gas}} - E_{s,\text{gas}})$) on the dielectric constant of the solvent (Table 1).

For the PCM method $\Delta(\Delta E_{e-s,\text{solv}})$ becomes more negative with increasing dielectric constant, although the trend is less pronounced when using the CAM-B3LYP functional which better models longer range interactions. Although the CPCM method predicts that the eclipsed form is relatively more stable in all solvents, and this is more pronounced for solvents with a larger dielectric constant, there is only a weak correlation between $\Delta(\Delta E_{e-s,\text{solv}})$ and the dielectric constant. There is no clear predicted dependence of $\Delta(\Delta E_{e-s,\text{solv}})$ on the dielectric constant for the SMD calculations. For solvents with a small dielectric constant the eclipsed form is calculated to be comparatively more stable with the introduction of solvation on going from PCM to CPCM to SMD models. In the cases where the COSMO model (Klamt and Schuurmann, 1993; Klamt, 1995; Klamt and Jonas, 1996; Pye and Ziegler, 1999) has

Table 1

Theoretical solvent and solvation model dependence of the excess energy difference between the eclipsed (D_{5h}) and staggered (D_{5d}) rotamers of Fc in solutions.*

Solvent (ϵ_r)	$\Delta(\Delta E_{e-s,\text{solv}})$ ($\text{kcal}\cdot\text{mol}^{-1}$)				
	PCM ^a	PCM ^b	CPCM ^a	SMD ^a	COSMO ^c
Hex (1.89)	+0.04	+0.05	-0.05	-0.14	
CCl_4 (2.24)	+0.04	+0.08	-0.07	-0.19	-0.45
DOX (2.25)	+0.04	+0.05	-0.06	-0.21	
THF (7.52)	-0.02	+0.03	-0.10	+0.05	
DCM (8.93)	-0.03	+0.02	-0.11	+0.06	
ACN (36.64)	-0.09	0.00	-0.10	-0.13	-0.48

* $\Delta(\Delta E_{e-s,\text{solv}}) = (E_{e,\text{solv}} - E_{s,\text{solv}}) - (E_{e,\text{gas}} - E_{s,\text{gas}}) = \Delta E_{e-s,\text{solv}} - \Delta E_{e-s,\text{gas}}$.

^a B3LYP/m6-31G(d) model in Gaussian. $\Delta E_{e-s,\text{gas}} = -0.58 \text{ kcal}\cdot\text{mol}^{-1}$.

^b CAM-B3LYP/m6-31G(d) model in Gaussian. $\Delta E_{e-s,\text{gas}} = -0.60 \text{ kcal}\cdot\text{mol}^{-1}$.

^c COSMO solvent model (Klamt and Schuurmann, 1993; Klamt, 1995; Klamt and Jonas, 1996; Pye and Ziegler, 1999) and B3LYP/TZ2P + model in ADF. $\Delta E_{e-s,\text{gas}} = -0.14 \text{ kcal}\cdot\text{mol}^{-1}$.

been applied, there is a larger solvation-based predicted preference for the D_{5h} conformer. This may be slightly more pronounced in more polar solvents.

In addition to solvation, longer-range Van der Waals interactions may also contribute to the barrier for ring rotation in Fc. These effects

may be calculated by inclusion of long range and dispersion correction to the DFT functional, such as B3LYP-D3, CAM-B3LYP and CAM-B3LYP-D3 functionals etc. However, we found that corrections of this sort did not make significant changes to the geometry, form of the spectra or the relative energy differences of the Fc D_{5h} and D_{5d} conformers for the

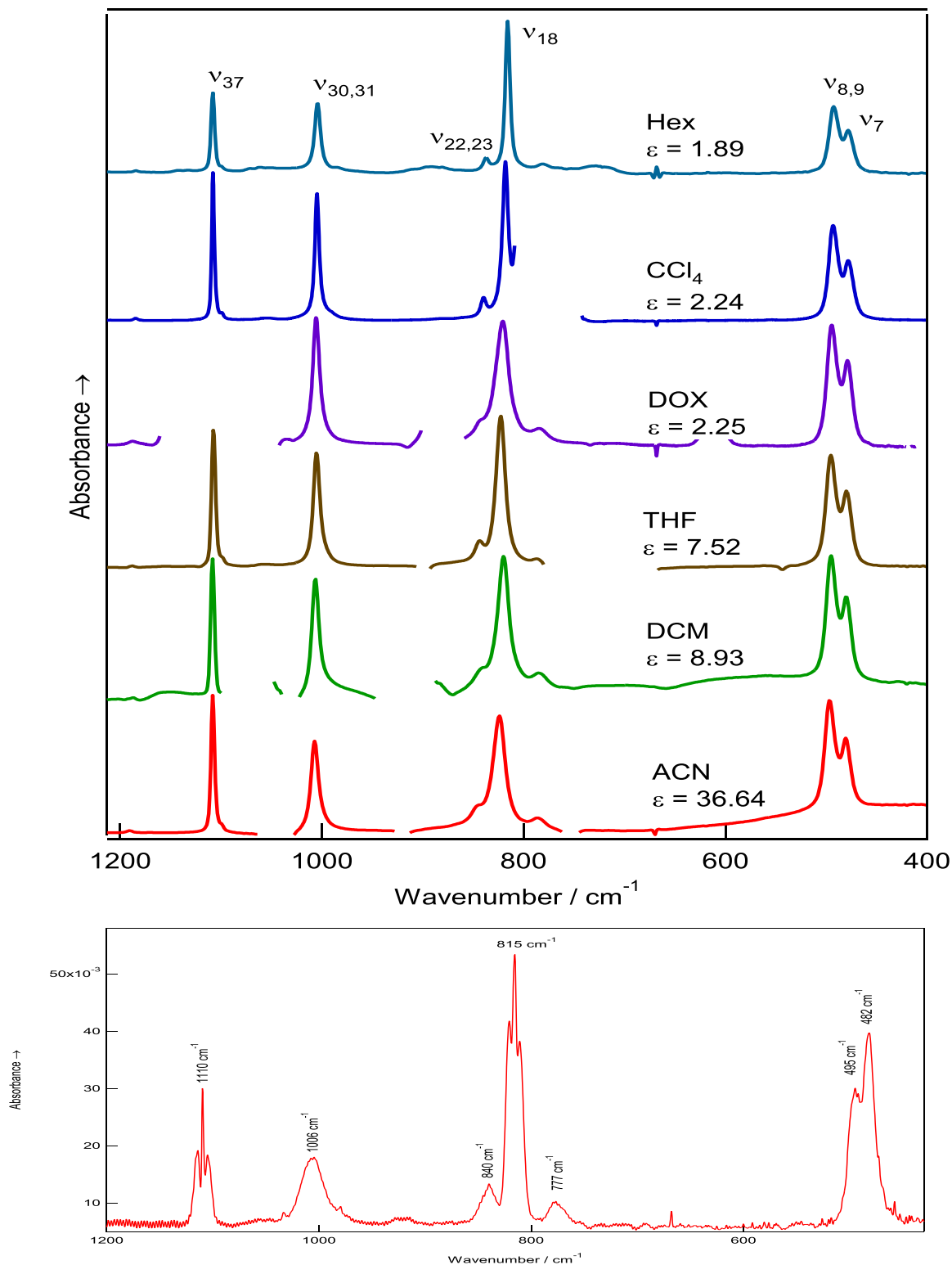


Fig. 1. Top: Redrawn room temperature measured solution IR spectra of Fc for the solvents under computational investigation (Hex = n-hexane, CCl_4 = carbon tetrachloride, DOX = 1,4 dioxane, THF = tetrahydrofuran, DCM = dichloromethane, ACN = acetonitrile) from Wang et al. (2021) and Best et al. (2016). The spectra are ordered according to the dielectric constant (ϵ) of the solvent and the discontinuities in the observed spectra are due to interference caused by strong solvent absorption. Bottom: the measured IR spectrum of Fc in gas phase (Best et al., 2016).

solvated species. For example, the $\Delta(\Delta E_{e-s, \text{solv}})$ values range from +0.04 to +0.08 kcal mol⁻¹ in CCl₄ solution (PCM), calculated using B3LYP, B3LYP-D3, CAM-B3LYP and CAM-B3LYP-D3 functionals and m6-31G(d) basis sets (Table S3).

3.2. Solvent effects on Fc conformers

Fig. 1 and Table 2 compares the measured IR spectra of Fc in solvents in the region of 400–1200 cm⁻¹ under room temperature in the present study. Table 2 also compares the present measurement with other available measurements in the literature. The last two columns are from the seminal IR measurement of Lippincott and Nelson (Lippincott and Nelson, 1958) in gas phase (vapor at 120 °C) and CCl₄ solution at room temperature (25 °C), respectively. The spectra in this region are dominated by six bands (ν_7 , $\nu_{8,9}$, ν_{18} , $\nu_{22,23}$, $\nu_{30,31}$ and ν_{37}) which are labelled following the order of normal modes from gas-phase DFT calculations of Fc (in eclipsed form D_{5h}) (Mohammadi et al., 2012). The last columns of Table 2 give the early measurements in gas phase and CCl₄ solution of Lippincott and Nelson (1958) for comparison. As expected, there is a good agreement with reports of the solution spectra of Fc (Lippincott and Nelson, 1958; Duhovic and Diaconescu, 2013) and there are comparatively modest shifts in the wavenumbers and integrated intensities of the different modes for the full range of solvents or for the gas phase species (Fischer and Pfab, 1952; Wang et al., 2021; Best et al., 2016).

As seen from the results that the major IR bands and their positions in this region the present measurements agree well with earlier measurements of Lippincott and Nelson (1958). The Fc IR spectra in gas phase and CCl₄ solvent undertaken in the present study are virtually identical to corresponding earlier measurements of Lippincott and Nelson (1958). The largest discrepancies in CCl₄ solvent between two measurements are ν_{18} and $\nu_{22,23}$, which differ by 6–7 cm⁻¹. It is noted that the present IR measurements are assisted by theoretical calculations whereas the earlier Lippincott and Nelson (1958) measurements were without such assistance. It is also seen in Table 2 that the IR spectra do not exhibit noticeable differences in gas phase and in solvents, except for the profiles of bands ν_7 and $\nu_{8,9}$ in the region of 480–500 cm⁻¹, which also agree with the Lippincott and Nelson (1958) measurements. Most of IR band positions in solvents are within ± 5 cm⁻¹ of the corresponding gas phase positions. Such the discrepancy is close to the error bars of the spectrometers (most spectrometers at room temperature exhibit a spectral resolution of 4 cm⁻¹). However, as reported in Fig. 1, the most noticeable difference in IR spectra between gas phase and solvents is not band positions but band profile of bands ν_7 and $\nu_{8,9}$ in the region of 480–500 cm⁻¹.

Table 3 reports the calculated six IR band positions and their deviations from the measurement of the eclipsed Fc in the region of 400–1200 cm⁻¹. The fully calculated IR spectra of Fc (100–3300 cm⁻¹) in CCl₄ solvent are assigned and given in Table S2. The PCM solvent model is employed in following calculations as the PCM model give

Table 2

Solvent dependence of the measured wavenumbers of the IR-active modes of Fc in the region 400 to 1200 cm⁻¹ and their comparison with the gas phase measurements (cm⁻¹).*

Band	ACN	DCM	THF	DOX	CCl ₄	Hex	Gas	Gas ²⁰	CCl ₄ ²⁰
$\epsilon_r = \epsilon/\epsilon_0$	36.64	8.93	7.52	2.25	2.24	1.89			2.2
ν_7	481 (-1)	480 (-2)	480 (-2)	479 (-3)	478 (-4)	478 (-4)	482	480	478
$\nu_{8,9}$	497 (2)	496 (1)	495 (0)	495 (0)	493 (-2)	493 (-2)	495	496	492
ν_{18}	824 (9)	820 (5)	822 (7)	821 (6)	818 (3)	816 (1)	815	816	811
$\nu_{22,23}$	844 (4)	840 (0)	844 (4)	844 (4)	840 (0)	837 (-3)	840	840	834
$\nu_{30,31}$	1007 (1)	1007 (1)	1006 (0)	1006 (0)	1005 (-1)	1004 (-2)	1006	1012	1002
ν_{37}	1108 (-2)	1108 (-2)	1108 (-2)	— (-)	1108 (-2)	1108 (-2)	1110	1112	1108

* Measurements were performed at room temperature (see Refs (Fischer and Pfab, 1952; Wang et al., 2021) and (Best et al., 2016)). The shifts, $\Delta\nu = \nu_{\text{solvent}} - \nu_{\text{gas}}$, are in parentheses. Mode labels are given in order of the DFT-calculated normal modes for the D_{5h} conformer of Fc in the gas phase. (Best et al., 2016) The experimental wavenumbers are within experimental error (1–2 cm⁻¹) of published spectra aside from a single report where the $\nu_{22,23}$ band is given, incorrectly, at 834 cm⁻¹. (Duhovic and Diaconescu, 2013).

Table 3

Calculated IR spectral band wavenumbers (cm⁻¹) of PCM-solvated Fc (eclipsed conformer) and comparison with the observed spectra.

Model	$\nu_{\text{calc}} (\Delta\nu)^a$ (B3LYP/m6-31G(d))							
	Solvent (ϵ_r)	ACN	DCM	THF	DOX	CCl ₄	Hex	Gas
ν_7	467	468	468	469	469	470	471	
	(-14)	(-12)	(-12)	(-10)	(-9)	(-8)	(-11)	
$\nu_{8,9}$	485	486	486	487	487	488	488	
	(-12)	(-10)	(-9)	(-8)	(-6)	(-5)	(-7)	
ν_{18}	845	845	845	844	844	844	844	
	(21)	(25)	(23)	(23)	(26)	(28)	(29)	
$\nu_{22,23}$	865	866	866	868	869	869	870	
	(21)	(26)	(22)	(24)	(29)	(32)	(30)	
$\nu_{30,31}$	1030	1030	1031	1032	1032	1034	1035	
	(23)	(23)	(25)	(26)	(27)	(30)	(29)	
ν_{37}	1134	1135	1135	1137	1137	1140	1141	
	(26)	(27)	(27)	(-)	(29)	(32)	(31)	
RMSD	20.1	21.6	20.8	19.7 ^b	23.1	25.2	24.9	
	$\nu_{\text{calc}} (\Delta\nu)^a$ (CAM-B3LYP/m6-31G(d))							
ν_7	484	486	486	487	486	487	488	
	(3)	(6)	(6)	(8)	(8)	(9)	(6)	
$\nu_{8,9}$	505	506	506	507	507	507	508	
	(8)	(10)	(11)	(12)	(14)	(14)	(13)	
ν_{18}	864	861	861	861	863	861	860	
	(40)	(41)	(39)	(40)	(45)	(45)	(45)	
$\nu_{22,23}$	885	886	887	889	889	889	890	
	(41)	(46)	(43)	(45)	(49)	(52)	(50)	
$\nu_{30,31}$	1045	1046	1046	1048	1048	1048	1049	
	(38)	(39)	(40)	(42)	(43)	(43)	(43)	
ν_{37}	1160	1161	1160	1063	1163	1163	1165	
	(52)	(53)	(52)	(-)	(55)	(55)	(55)	
RMSD	32.7	34.4	33.5	30.5 ^b	37.0	37.6	37.0	

^a The deviation of the calculated and observed wavenumbers, (Fischer and Pfab, 1952; Wang et al., 2021; Best et al., 2016) $\Delta\nu = \nu_{\text{calc}} - \nu_{\text{exp}}$, is given in parentheses.

^b Based on the five observed IR bands.

geometries with less distortion from the high-symmetry D_{5h} and D_{5d} forms. Note that the companion article used the SMD model in the same issue (Fischer and Pfab, 1952; Wang et al., 2021). This table also compares the impact of the DFT functionals on the calculated IR spectra of Fc, in which the B3LYP and CAM-B3LYP methods contain different treatment of longer range interactions translates. It is reported in Table 3 that a blue shift for all calculated frequencies of the vibrational modes from the corresponding measurements when calculated using the CAM-B3LYP method. The root-mean square deviation (RMSD) of the calculated IR bands in Table 3 (30–37 cm⁻¹). On the other hand, the B3LYP method exhibits shifts in opposite directions of red-shift for the vibrational modes (ν_7 and $\nu_{8,9}$) under 500 cm⁻¹ and blue shift for the modes (ν_{18} - ν_{37} modes) above 500 cm⁻¹, with an apparently smaller RMSD of 20–25 cm⁻¹. The opposite shifts suggest the bonding natures of ν_7 and $\nu_{8,9}$ modes are different from other modes.

Analysis of the IR band profile of the ν_7 and $\nu_{8,9}$ modes provides an ideal illustration of the reaction coordinate method (RCM) based on the quantum mechanically calculated IR spectra of the D_{5h} and D_{5d} rotamers (Best et al., 2016; Trevorah et al., 2020) and $\Delta E_{e-s,solv}$. This approach assumes that the reaction surface for the relative rotation of the Cp rings has low and high energy limits corresponding to the D_{5h} and D_{5d} geometries and produces the temperature dependent spectra in gas phase with band profiles reflecting the Boltzmann population of the vibrational levels of the reaction coordinate (Best et al., 2016; Trevorah et al., 2020) and estimating the energy difference between the D_{5h} and D_{5d} rotamers of Fc. The gas phase calculated spectra were shown to provide the necessary information where the approach was tested by modelling of the temperature dependence of the IR spectra. The extension of the approach to the different solvents considered in this investigation requires a robust calculation of the IR spectra. While we have shown that there are differences in the calculated wavenumbers of the ν_7 and $\nu_{8,9}$ modes for a given basis set depending on the functional and solvation model, the energy difference between these modes is comparatively insensitive to those features of the calculation. The value of $\nu_{8,9} - \nu_7$ is 18 cm^{-1} for all solvents with the B3LYP functional and $20 \pm 1 \text{ cm}^{-1}$ for CAM-B3LYP calculations as reported in Table 3. It suggests that the B3LYP/PCM calculations may be used to provide the band profiles for the D_{5h} and D_{5d} Fc rotamers.

The RCM estimated band profiles for Fc at room temperature in the different solvents are shown in Fig. 2b (dotted line). The values of $\Delta E_{e-s,solv}$ and the spectra of the D_{5h} and D_{5d} rotamers were obtained from B3LYP/m-631G(d,p) calculations with the PCM model. Using the predicted energy separation of the conformers by B3LYP/m-631G(d,p) calculations clearly yields a poor match to experiment. Fig. 2 shows that a much larger value (ca. $1.8 \text{ kcal}\cdot\text{mol}^{-1}$) of $\Delta E_{e-s,solv}$ is required to modestly represent the observed spectra (Fig. 2a, solid line). This has followed the empirical estimation for RCM following Ref (Best et al., 2016); more accurate work would follow the hypothesis-testing analysis of Ref (Trevorah et al., 2020), yet would still yield the same qualitative conclusion that the conformer gap is well underestimated by current

theory. Whilst small differences in the values of $\Delta E_{e-s,solv}$ for the different solvents are plausible, more reliable estimates of the energy difference require measurement of the spectra over a more extended temperature range like in the gas phase (Best et al., 2016), and in condensed phases (Trevorah et al., 2020). Nonetheless, the comparative insensitivity of $\Delta E_{e-s,solv}$ on the dielectric constant of the solvent is supported by the analysis. This suggests that the implicit solvent models employed in this study may be not sufficient to produce the energy barrier of the Fc conformer in solutions. Further explicit solvent models and molecular dynamics simulations in solvent will provide more information in this direction, which is out of the scope of the present study.

3.3. Energy decomposition analysis (EDA)

In order to understand the nature of the Fc energy contributions to the configurations in solutions, we further investigate Fc conformers in solvents using EDA (von Hopffgarten and Frenking, 2012), which was applied to study Fc conformers in gas phase (Wang et al., 2015). The calculations in solvent are the same (i.e., the B3LYP/TZ2P+) model in ADF as in gas phase (Wang et al., 2015), except that the solvent model is based on the COSMO solvent model (Klamt and Schuurmann, 1993; Klamt, 1995; Klamt and Jonas, 1996; Pye and Ziegler, 1999). It results in a solvation-based preference of interaction energy for the eclipsed (D_{5h}) conformer of ca. $0.59 \text{ kcal}\cdot\text{mol}^{-1}$ in CCl_4 and $0.62 \text{ kcal}\cdot\text{mol}^{-1}$ in ACN relative to the same conformer (D_{5h}) in gas phase. The calculations, however, using the B3LYP/TZ2P+ model in ADF is not exactly the same model in the Gaussian program, although very similar Slater basis set (TZ2P+) is employed for the m6-31G(d) Gaussian basis set. The obtained Fc conformer energy difference for $\Delta E_{e-s,gas}$ of $-0.14 \text{ kcal}\cdot\text{mol}^{-1}$ in gas phase is smaller but in the same trend for more stable D_{5h} conformer.

Previous EDA of isolated Fc (gas phase) by Wang and coworkers (Wang et al., 2015) demonstrated that the partitioning of the interaction energy ΔE_{int} of Fc conformers into ΔE_{elstat} , ΔE_{Pauli} , and ΔE_{orb} contributions is highly sensitive to the fragmentation schemes. In other word,

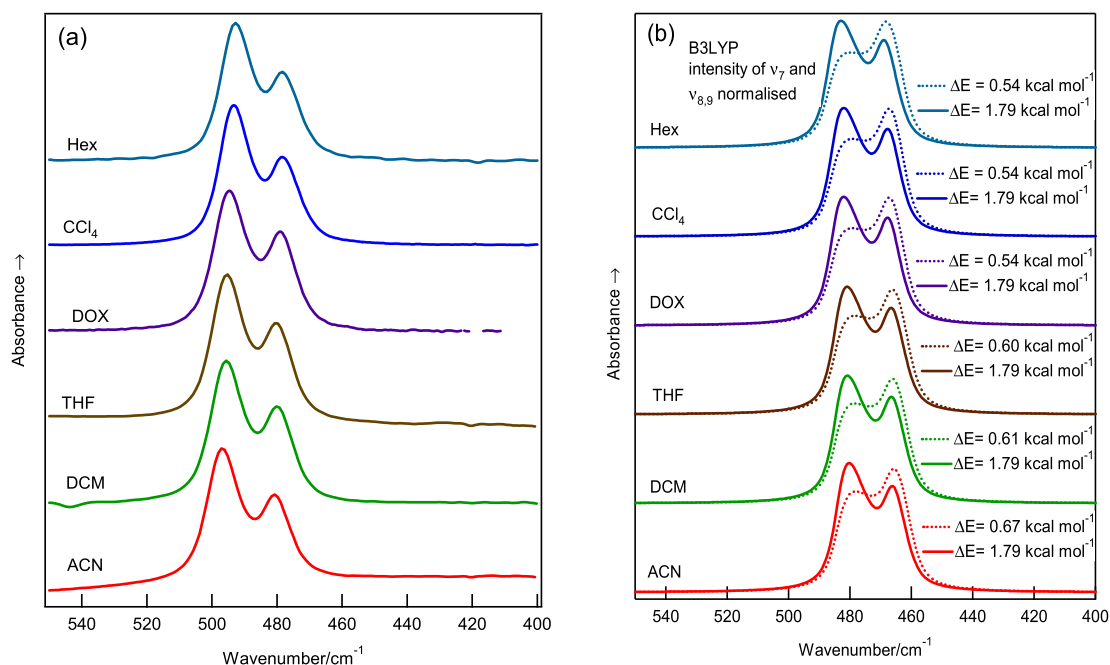


Fig. 2. IR spectra of Fc in solution in the region $400\text{--}550 \text{ cm}^{-1}$. (a) experimental spectra (Fischer and Pfab, 1952; Wang et al., 2021; Best et al., 2016). (b) RCM calculated band profiles using DFT energy difference of PCM-solvated D_{5h} and D_{5d} forms of Fc, ν_7 was set to 20 cm^{-1} , full width at half maximum set to 7 cm^{-1} and the energy difference (ΔE) between PCM-solvated D_{5h} and D_{5d} was set either to the PCM model-predicted value (Table 2, $|\Delta(\Delta E_{e-s,so})|$), dotted line, or set to the larger value of $1.79 \text{ kcal}\cdot\text{mol}^{-1}$ (solid lines). This implementation of RCM is approximate and empirical, following Ref. (Best et al., 2016) and indicates that approximate agreement can be obtained with the RCM approach yet requires a significantly larger conformer separation than theoretically predicted to date, which would be expected also from more advanced RCM analysis (Trevorah et al., 2020).

the EDA energy components are not uniquely defined quantities and are path functions (Andrada and Foroutan-Nejad, 2020). Nevertheless, EDA is a useful tool to compare the nature of bonds in closely related structures such as Fc. In the absence of universally accepted reference states, it is discovered that the neutral atom fragment scheme resulted in a partitioning of the energies of Fc gives an internally consistent distribution of interaction energy which converge on the results from accurate DFT models. The finding of more stable D_{5h} conformer of Fc in gas phase (Wang et al., 2015) is confirmed by a recent study (Vlahovic et al., 2017) using the OPBE/TZP model with ZORA (Lenthe et al., 1993) scalar relativistic corrections, as well as recent molecular dynamics (MD) simulations of Fc (Wang and Vasilyev, 2020). The impact of solvation on the energy components is illustrated by calculations conducted in a non-polar solvent CCl_4 and a polar solvent ACN using the same fragmentation scheme and theory employed for the gas-phase species (Wang et al., 2015).

The calculated energy contributions to the relative conformer energy term $\Delta(\Delta E_{e-s})$ with the component energy values for the different conformers are available in Table 4 in CCl_4 and ACN solvents. The calculated energy components (ΔE_{e-s}) of eclipsed and staggered Fc conformers in CCl_4 and ACN solvents are given in Table S4. The previously reported EDA values for gas phase Fc (Wang et al., 2015) are included for reference. The overall interaction energy is reported as ΔE_{int} and the signs of the relative energy $\Delta E_{int(e-s)}$ reveal that the eclipsed (D_{5h}) Fc is the more stable conformer when negative or the staggered (D_{5d}) Fc is the more stable conformer when positive. Although the trend of the interaction energy $\Delta E_{int(e-s)}$ is the same in gas phase and in solutions as shown in Table 4 prefers eclipsed Fc (i.e., $\Delta E_{int(e-s)} < 0$), this preference becomes more pronounced with solvation. For example, $\Delta E_{int(e-s)}$ in gas phase is $-0.14 \text{ kcal}\cdot\text{mol}^{-1}$ (in this model), this interaction energy is enhanced over three times to $-0.59 \text{ kcal}\cdot\text{mol}^{-1}$ in CCl_4 and $-0.62 \text{ kcal}\cdot\text{mol}^{-1}$ in ACN solvents using the same method.

The interaction energy within the EDA framework contains three major energy components (neglecting the dispersion energy). As reported in Table 4, in gas phase the small interaction energy comes from cancellation of different energy components between the electrostatic energy ΔE_{estat} ($-2.23 \text{ kcal}\cdot\text{mol}^{-1}$) and orbital energy ΔE_{orb} ($2.55 \text{ kcal}\cdot\text{mol}^{-1}$), whereas the quantum mechanical Pauli energy ΔE_{Pauli} is very small ($-0.46 \text{ kcal}\cdot\text{mol}^{-1}$), although the interaction energy is negative preferring the D_{5h} Fc conformer (Wang et al., 2015). In solvents such as CCl_4 , however, the cancellations are between the quantum mechanical Pauli energy ΔE_{Pauli} ($-5.78 \text{ kcal}\cdot\text{mol}^{-1}$) and orbital energy ΔE_{orb} ($5.28 \text{ kcal}\cdot\text{mol}^{-1}$) and a small electrostatic energy ΔE_{estat} ($-0.06 \text{ kcal}\cdot\text{mol}^{-1}$).

Table 4

Comparison of changes in energy components ($\text{kcal}\cdot\text{mol}^{-1}$) for the eclipsed (D_{5h}) and staggered (D_{5d}) ferrocene in CCl_4 and ACN solvation using the COSMO model.^{a,*,†}

Terms	$\Delta\Delta E_{e-s}$ (gas) ^b	$\Delta\Delta E_{e-s}$ (CCl_4)	$\Delta\Delta E_{e-s}$ (ACN)	$\Delta\Delta E_e$ (CCl_4)	$\Delta\Delta E_s$ (CCl_4)	$\Delta\Delta E_c$ (ACN)	$\Delta\Delta E_p$ (ACN)
ΔE_{estat}	-2.23	-0.06	-0.07	3.44	1.27	6.08	3.92
ΔE_{Pauli}	-0.46	-5.78	-5.68	-18.84	-13.52	-34.38	-29.16
ΔE_{orb}	2.55	5.28	5.17	15.07	12.34	28.35	25.73
$\Delta E_{sol}^{\ddagger}$	0.0	-0.03	-0.04	-1.05	-1.02	-2.50	-2.46
ΔE_{int}^c	-0.14	-0.59	-0.62	-1.38	-0.93	-2.45	-1.97
ΔE_{ster}	-2.69	-5.84	-5.75	-15.40	-12.25	-28.30	-25.24

* Using the COSMO model (Klamt and Schuurmann, 1993; Klamt, 1995; Klamt and Jonas, 1996; Pye and Ziegler, 1999) and the B3LYP/TZ2P + model in ADF.

† All energies are given in $\text{kcal}\cdot\text{mol}^{-1}$; The fragment scheme is $Fe(C_5H_5)_2 \rightarrow Fe$ ((3d) (Coriani et al., 2006), singlet) + 10 C ((2p) (Wilkinson et al., 1952), singlet) + 10 H ((1s) (Fischer and Pfab, 1952), doublet). Here ΔE_{estat} , ΔE_{Pauli} , ΔE_{orb} and ΔE_{ster} ($=\Delta E_{estat} + \Delta E_{Pauli}$).

^b Results in gas phase from Wang et al. (2015).

^c $\Delta E_{int} = \Delta E_{estat} + \Delta E_{Pauli} + \Delta E_{orb} + \Delta E_{sol}$.

^d $\Delta\Delta E_{e-s,solv} = \Delta\Delta E_{e,solv} - \Delta\Delta E_{s,solv}$, where $\Delta\Delta E_{e,solv} = \Delta E_{e,solv} - \Delta E_{e,gas}$ and $\Delta\Delta E_{s,solv} = \Delta E_{s,solv} - \Delta E_{s,gas}$.

The nature of the energy component contributions to the interaction energy is not the same in gas phase and in solution in Table 4. Within the EDA framework, the interaction energy (ΔE_{in}) is defined as the energy difference between the electronic energy of a whole molecular system and the sum of the energies of its fragments in their geometry and reference electronic state within the system, which may or may not be their ground electronic state (Andrada and Foroutan-Nejad, 2020). The usually attractive electrostatic energy ΔE_{estat} term corresponds to the classical electrostatic interaction between the unperturbed charge distributions of the geometrically deformed (prepared) interacting atoms (fragments). The electrostatic energy difference $\Delta\Delta E_{e-s}$ between the eclipsed and staggered Fc in gas phase and in solvent (CCl_4) $-2.23 \text{ kcal}\cdot\text{mol}^{-1}$ and $-0.06 \text{ kcal}\cdot\text{mol}^{-1}$, respectively, in favour of the eclipsed Fc. It suggests that solvent effect contributes to reduction of the differences in classical electrostatic interactions of the Fc conformers by approximately $2.17 \text{ kcal}\cdot\text{mol}^{-1}$.

The Pauli repulsion ΔE_{Pauli} term is the energy change associated with the transformation from the superposition of the unperturbed wave functions (Slater determinant of the Kohn–Sham orbitals) of the isolated fragments to the wave function. Alternatively exchange repulsion, or overlap repulsion, accounts for the unfavourable interaction of overlapping filled orbitals between the fragments. A quantum mechanical term which refers to Pauli principle through explicit anti-symmetrisation and renormalisation of the product wave function. It comprises the destabilizing interactions between electrons of the same spin on the fragments. This term in gas phase $\Delta\Delta E_{e-s}$ is given by $-0.46 \text{ kcal}\cdot\text{mol}^{-1}$ slightly in favour of the eclipsed Fc but this term becomes $-5.78 \text{ kcal}\cdot\text{mol}^{-1}$ (CCl_4), which is over 10 times more than the gas phase in favour of the eclipsed Fc.

The orbital interaction ΔE_{orb} accounts for charge transfer between the occupied and empty orbitals of the two fragments and polarization that is charge reorganization within each fragment. This orbital interaction in gas phase $\Delta\Delta E_{e-s}$ is given by $2.55 \text{ kcal}\cdot\text{mol}^{-1}$ in favour of the staggered Fc but this term becomes $5.28 \text{ kcal}\cdot\text{mol}^{-1}$ (CCl_4), which is over twice larger in favour of the staggered Fc in solvent. As a result, it indicates that solvent resists charge transfer between the occupied and empty orbitals of the eclipsed more than in staggered Fc.

As a result, Table 4 and Fig. 3 reveals that the solvent effect results in an apparent increase (nearly doubled) of steric energy, which is the sum of electrostatic energy and quantum mechanical Pauli energy ($\Delta E_{ster} = \Delta E_{estat} + \Delta E_{Pauli}$), from $-2.69 \text{ kcal}\cdot\text{mol}^{-1}$ in gas phase to over $-5.75 \text{ kcal}\cdot\text{mol}^{-1}$ in solutions. The electrostatic energy and Pauli quantum mechanical energy contribute approximately 42.6% and 8.7%, respectively, to the total energy in gas phase. The same energy contributions become approximately 0.5% and 52%, respectively, in CCl_4 solution. An additional solvation energy term, ΔE_{sol} , which is introduced as the energy reduced from the gas phase, indicates that solvent enhances the stability of the Fc conformers. The ΔE_{sol} term reflects the interaction between the charge distribution of the Fc molecule (solute) and the charge distribution of the cavity (solvent environment).

Examination of the calculations, by comparing the differences in the energy component terms reveals clearly the impact of solvation favouring the eclipsed Fc conformer (ΔE_{estat} and ΔE_{Pauli}) over the staggered Fc conformer (ΔE_{orb}) conformer in Table 4. The eclipsed form exhibits larger energy changes from gas phase for all the energy components than the staggered form. Almost doubled steric energy value of $\Delta(\Delta E_{ster})$ in solutions ($-5.84 \text{ kcal}\cdot\text{mol}^{-1}$ in the CCl_4 solvent and $-5.75 \text{ kcal}\cdot\text{mol}^{-1}$ in the ACN solvent) with respect to the gas phase ($-2.69 \text{ kcal}\cdot\text{mol}^{-1}$) is observed, indicating that the eclipsed Fc is stabilized in solutions significantly than in the gas phase. The electrostatic energy (ΔE_{estat}) reduces from $-2.23 \text{ kcal}\cdot\text{mol}^{-1}$ in gas phase to $-0.06 \text{ kcal}\cdot\text{mol}^{-1}$ in CCl_4 solution, and the value of quantum mechanical Pauli energy (ΔE_{Pauli}) increases (value) from $-0.46 \text{ kcal}\cdot\text{mol}^{-1}$ in gas phase to $-5.76 \text{ kcal}\cdot\text{mol}^{-1}$ in CCl_4 solvent, although conversely the orbital interaction (ΔE_{orb}) is less favourable for the solvated Fc, from $2.55 \text{ kcal}\cdot\text{mol}^{-1}$ in gas phase to $5.28 \text{ kcal}\cdot\text{mol}^{-1}$ in CCl_4 . As a result, a net

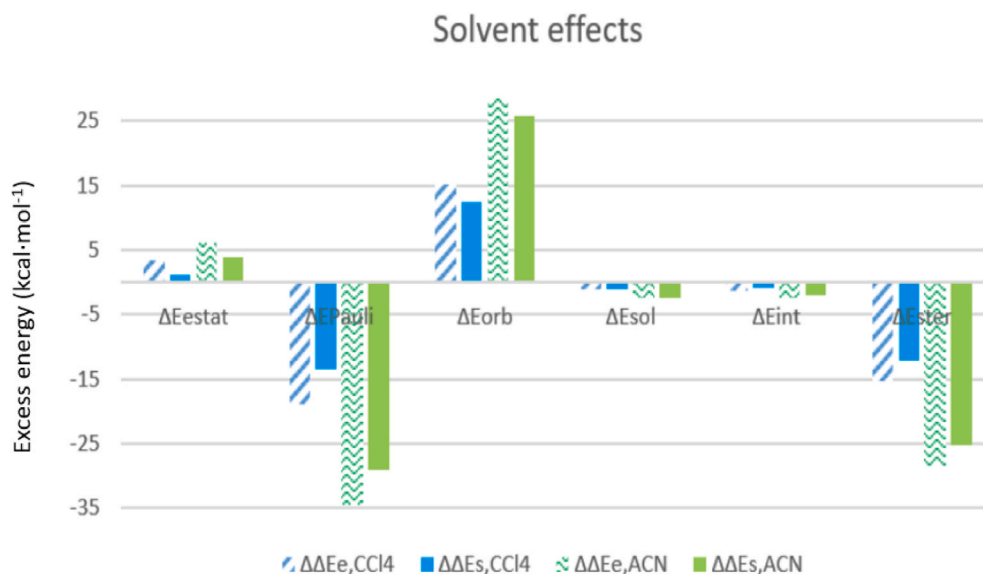


Fig. 3. Excess energies (kcal·mol⁻¹) of Fc energy components in solvent with respect to their gas phase counterparts. Blue for CCl₄ solvent and green for ACN solvent. Pattern for eclipsed and solid for staggered (Data from right hand side of Table 4).

negative solvation energy change (ΔE_{sol}) of -0.03 kcal·mol⁻¹ in CCl₄ or -0.04 kcal·mol⁻¹ in ACN further stabilizes the eclipsed conformer in solutions.

4. Conclusions

The present study uses the solvent Fc IR measurement validated theoretical methods to investigate contributions of eclipsed and staggered conformers of Fc to the IR profile differences (in the region 400–500 cm⁻¹) in a number of solvents from gas phase. The IR spectral calculations using DFT based B3LYP, its long-range (CAM-B3LYP) and dispersion corrections (CAM-B3LYP-D3) derivatives with appropriate basis set (m6-31G(d,p)), applying the polarizable continuum solvation model (PCM) agree well with the measurements in a number of solvents in the region 400–1200 cm⁻¹. Several solvation models are examined with respect to the IR spectra. It is found that the PCM model shows consistent changes in solvent and the impact of solvent polarity is small.

Solvent impacts on ferrocene configuration and the nature of its component energies, however.

Further analysis of the vibrational modes in the 480–500 cm⁻¹ region (ν_7 , $\nu_{8,9}$) using the reaction coordinate model suggests that the energy difference (ΔE_{e-s}) between the Fc conformers may be underestimated by implicit solvent model in the calculations. Further investigation in this direction such as advanced RCM analysis (Trevorah et al., 2020), explicit solvent model and solvent molecular dynamics simulations is warranted. The impact of solvation on Fc conformers is further investigated using energy decomposition analysis (EDA) in a non-polar (tetrachloromethane (CCl₄)) and a polar (acetonitrile (ACN)) solvent. It is suggested that solvation changes the electrostatic and quantum mechanical Pauli energy contributions to the interaction energy of Fc conformers, which result in a large steric energy in solvents so that to enhance the dominance of the eclipsed Fc, an observation consistent with the analysis of the bands due to the ν_7 , $\nu_{8,9}$ modes.

Declaration of competing interest

The authors declare that they have no known competing financial interests or personal relationships that could have appeared to influence the work reported in this paper.

Acknowledgements

We acknowledge Swinburne University Supercomputing Facilities. SI acknowledges Swinburne University Postgraduate Research Award (SUPRA). The gas-phase spectroscopy was undertaken on the THz/Far-IR beamline at the Australian Synchrotron, Victoria, Australia, Dr Dominique Appadoo is thanked for his assistance with those gas phase measurements. Finally, the authors would like to acknowledge Dr Stephen Best for producing Figs. 1 and 2 and useful discussions to the revision of the manuscript.

Appendix A. Supplementary data

Supplementary data related to this article can be found at <https://doi.org/10.1016/j.radphyschem.2021.109697>.

References

- Amovilli, C., Barone, V., Cammi, R., Cancès, E., Cossi, M., Mennucci, B., Pomelli, C.S., Tomasi, J., 1998. Recent advances in the description of solvent effects with the polarizable continuum model. *Adv. Quant. Chem.* 32, 227–261.
- Andrada, D.M., Foroutan-Nejad, C., 2020. Energy components in energy decomposition analysis (EDA) are path functions; why does it matter? *Phys. Chem. Chem. Phys.* 22 (39), 22459–22464.
- Appel, M., Frick, B., Spehr, T.L., Stuhn, B., 2015. Molecular ring rotation in solid ferrocene revisited. *J. Chem. Phys.* 142, 114503.
- Baerends, E.J., Ziegler, T., Atkins, A.J., Autschbach, J., Bashford, D., Bérces, A., Bickelhaupt, F.M., Bo, C., Boerrigter, P.M., Cavallo, L., et al., 2016. ADF2016, SCM, Theoretical Chemistry. Vrije Universiteit, Amsterdam, The Netherlands.
- Barone, V., Cossi, M., 1998. Quantum calculation of molecular energies and energy gradients in solution by a conductor solvent model. *J. Phys. Chem. A* 102, 1995–2001.
- Best, S.P., Wang, F., Islam, M.T., Islam, S., Appadoo, D., Trevorah, R.M., Chantler, C.T., 2016. Reinterpretation of dynamic vibrational spectroscopy to determine the molecular structure and dynamics of ferrocene. *Chem. Eur. J.* 22, 18019–18026.
- Bohn, R.K., Haaland, A., 1966. On molecular structure of ferrocene Fe(C₅H₅)₂. *J. Organomet. Chem.* 5, 470–476.
- Bourke, J.D., Islam, M.T., Best, S.P., Tran, C.Q., Wang, F., Chantler, C.T., 2016. Conformation analysis of ferrocene and decamethylferrocene via full-potential modeling of XANES and XAFS spectra. *J. Phys. Chem. Lett.* 7, 2792–2796.
- Chantler, C.T., Rae, N.A., Islam, M.T., Best, S.P., Yeo, J., Smale, L.F., Hester, J., Mohammadi, N., Wang, F., 2012. Stereochemical analysis of ferrocene and the uncertainty of fluorescence XAFS data. *J. Synchrotron Radiat.* 19, 145–158.
- Chong, D.P., Van Lenthe, E., Van Gisbergen, S., Baerends, E.J., 2004. Even-tempered Slater-type orbitals revisited: from hydrogen to krypton. *J. Comput. Chem.* 25, 1030–1036.
- Coriani, S., Haaland, A., Helgaker, T., Jørgensen, P., 2006. The equilibrium structure of ferrocene. *ChemPhysChem* 7, 245–249.

- Cossi, M., Barone, V., 1998. Analytical second derivatives of the free energy in solution by polarizable continuum models. *J. Chem. Phys.* 109, 6246–6254.
- Cossi, M., Rega, N., Scalmani, G., Barone, V., 2003. Energies, structures, and electronic properties of molecules in solution with the C-PCM solvation model. *J. Comput. Chem.* 24, 669–681.
- Duhovic, S., Diaconescu, P.L., 2013. An experimental and computational study of 1,1'-ferrocene diamines. *Polyhedron* 52, 377–388.
- Dunitz, J.D., 1993. In forty years of ferrocene. *Verlag Helvetica Chim. Acta* 9–23.
- Dunitz, J.D., Orgel, L.E., 1955. Electronic structure of metal bis-cyclopentadienyls. *J. Chem. Phys.* 23, 954–958.
- Fischer, E.O., Pfab, W., 1952. Cyclopentadien-metallkomplexe, ein neuer typ metallorganischer verbindungen. *Z. Naturforsch.* B 7, 377–379.
- Frisch, M.J., Trucks, G.W., Schlegel, H.B., Scuseria, G.E., Robb, M.A., Cheeseman, J.R., Scalmani, G., Barone, V., Mennucci, B., Petersson, G.A., et al., 2009. *Gaussian 09, Revision E.01*, and *Gaussian 16*. Gaussian, Inc., Wallingford CT USA and 2016.
- Grimme, S., Antony, J., Ehrlich, S., Krieg, H., 2010. A consistent and accurate ab initio parametrization of density functional dispersion correction (DFT-D) for the 94 elements H-Pu. *J. Chem. Phys.* 132.
- Haaland, A., Nilsson, J.E., 1968. Determination of barrier to internal rotation in ferrocene and ruthenocene by means of electron diffraction. *Chem. Commun.* 88–89.
- Hao, R., Jia, N., Tian, G., Qi, S., Shi, L., Wang, X., Wu, D., 2018. Flash memory effects and devices based on functional polyimides bearing pendent ferrocene group. *Mater. Des.* 139, 298–303.
- Islam, M.T., Best, S.P., Bourke, J.D., Tantau, L.J., Tran, C.Q., Wang, F., Chantler, C.T., 2016. Accurate X-ray absorption spectra of dilute systems: absolute measurements and structural analysis of ferrocene and decamethyl ferrocene. *J. Phys. Chem. C* 120, 9399–9418.
- Islam, M.T., Trevorah, R.M., Appadoo, D.R.T., Best, S.P., Chantler, C.T., 2017. Methods and methodology for FTIR spectral correction of channel spectra and uncertainty, applied to ferrocene. *Spectrochim. Acta A* 177, 86.
- Kemner, E., de Schepper, I.M., Kearley, G.J., Jayasooriya, U.A., 2000. The vibrational spectrum of solid ferrocene by inelastic neutron scattering. *J. Chem. Phys.* 112, 10926–10929.
- Klamt, A., 1995. Conductor-like screening model for real solvents: a new approach to the quantitative calculation of solvation phenomena. *J. Phys. Chem.* 99, 2224–2235.
- Klamt, A., Jonas, V., 1996. Treatment of the outlying charge in continuum solvation models. *J. Chem. Phys.* 105, 9972–9981.
- Klamt, A., Schuurmann, G., 1993. COSMO: a new approach to dielectric screening in solvents with explicit expressions for the screening energy and its gradient. *J. Chem. Soc., Perkin Trans. 2*, 799–805.
- Kubo, A., Ikeda, R., Nakamura, D., 1981. Motion of C₅H₅ rings in three crystalline modifications of ferrocene as studied by ¹H-NMR. *Chem. Lett.* 1497–1500.
- Kubo, A., Ikeda, R., Nakamura, D., 1986. ¹H nuclear-magnetic-resonance studies on structural phase-transitions and molecular-dynamics of 5-membered rings in solid ferrocene, azaferrocene and ruthenocene. *J. Chem. Soc. Faraday. Trans. 2* (82), 1543–1562.
- Larik, F.A., Saeed, A., Fattah, T.A., Muqadar, U., Channar, P.A., 2017. Recent advances in the synthesis, biological activities and various applications of ferrocene derivatives. *Appl. Organomet. Chem.* 31, 3664–3685.
- Lenthe, E.v., Baerends, E.J., Snijders, J.G., 1993. Relativistic regular two-component Hamiltonians. *J. Chem. Phys.* 99 (6), 4597–4610.
- Lippincott, E.R., Nelson, R.D., 1958. The vibrational spectra and structure of ferrocene and ruthenocene. *Spectrochim. Acta* 10, 307–329.
- Marenich, A.V., Cramer, C.J., Truhlar, D.G., 2009. Universal solvation model based on solute electron density and on a continuum model of the solvent defined by the bulk dielectric constant and atomic surface tensions. *J. Phys. Chem. B* 113, 6378–6396.
- Mennucci, B., 2010. Continuum solvation models: what else can we learn from them? *J. Phys. Chem. Lett.* 1, 1666–1674.
- Mitin, A.V., Baker, J., Pulay, P., 2003. An improved 6-31G(*) basis set for first-row transition metals. *J. Chem. Phys.* 118, 7775–7782.
- Mohammadi, N., Ganesan, A., Chantler, C.T., Wang, F., 2012. Differentiation of ferrocene D_{5d} and D_{5h} conformers using IR spectroscopy. *J. Organomet. Chem.* 713, 51–59.
- Pietschnig, R., 2016. Polymers with pendant ferrocenes. *Chem. Soc. Rev.* 45, 5216–5231.
- Pye, C.C., Ziegler, T., 1999. An implementation of the conductor-like screening model of solvation within the amsterdam density functional package. *Theor. Chem. Acc.* 101, 396–408.
- Ribeiro, R.F., Marenich, A.V., Cramer, C.J., Truhlar, D.G., 2011. Use of solution-phase vibrational frequencies in continuum models for the free energy of solvation. *J. Phys. Chem. B* 115, 14556–14562.
- Seeman, J.I., Cantrill, S., 2016. Wrong but seminal. *Nat. Chem.* 8, 193–200.
- Seiler, P., Dunitz, J.D., 1979. A New interpretation of the disordered crystal structure of ferrocene. *Acta Crystallogr. B* B35, 1068–1074.
- Trevorah, R., Tran, N., Appadoo, D., Wang, F., Chantler, C.T., 2020. Resolution of ferrocene and deuterated ferrocene conformations using dynamic vibrational spectroscopy: experiment and theory. *Inorg. Chim. Acta.* 506, 11949.
- Vlahovic, F., Gruden, M., Swart, M., 2017. Rotating iron and titanium sandwich complexes. *Chem. Eur J.* <https://doi.org/10.1002/chem.201704829>.
- von Hopffgarten, M., Frenking, G., 2012. Energy decomposition analysis. *Wiley Interdiscip. Rev. Comput. Mol. Sci.* 2, 43–62.
- Wang, F., Vasilyev, V., 2020. Ferrocene conformation in low and higher temperatures: a molecular dynamics study. *Int. J. Quant. Chem.* 120, 1.
- Wang, F., Islam, S., Vasilyev, V., 2015. Ferrocene orientation determined intramolecular interactions using energy decomposition analysis. *Mater* 8, 7723–7737.
- Wang, F., Mohammadi, N., Best, S.P., Appadoo, D., Chantler, C.T., 2021. Dominance of eclipsed ferrocene conformer in solutions revealed by the IR spectra between 400 and 500 cm⁻¹, 109590 – 1 – 7 (this issue). *Radiat. Phys. Chem.* 188.
- Wilkinson, G., Rosenblum, M., Whiting, M.C., Woodward, R.B., 1952. The structure of iron bis-cyclopentadienyl. *J. Am. Chem. Soc.* 74, 2125–2126.
- Yanai, T., Tew, D.P., Handy, N.C., 2004. A new hybrid exchange-correlation functional using the coulomb-attenuating method (CAM-B3LYP). *Chem. Phys. Lett.* 393, 51–57.
- Yu, Y., Shi, D., 2017. Bio-gasoline Containing Additive and Manufacture Method and Application. CN107384490A.
- Zhao, H., Wang, Z., Gao, X., Wu, C., Liu, L., Liu, X., 2017. Simple Method for Directly Growing Carbon Nanotube Array on Metal to Realize Super-hydrophobic Modification, and its Application. CN107400928A.